Low temperature RNA

Author: Xavier Pérez Moré
*Facultat de Física, Universitat de Barcelona, Diagonal 645, 08028 Barcelona, Spain.**

Advisors: Jaime Aspas Cáceres and Félix Ritort Farrán
(Dated: June 23, 2021)

Abstract: We have used Optical Tweezers to mechanically stretch an RNA hairpin under different salt and temperature conditions, in order to analyze the effect of these parameters on its physical properties. Applying single-molecule force spectroscopy methods we study the presumably highly complex transition which qualitative agrees with the behaviour expected. Moreover, we have found a surprising intermediate state under the presence of Mg^{2+} ions at low temperature.

I. INTRODUCTION

In the last few years, biomedical and biotechnological developments have made evident the overwhelming advances in the scientific knowledge about biological systems and in the theoretical framework supporting non-equilibrium processes governing this biological world. We focus on RNA, which is implied in Biology at all levels. In its sequence it carries the genetic information encoding proteins. Beyond that, RNA folds in a huge variety of secondary structures, and can also be found as the main building block of the ribosome, the molecular machine where protein synthesis occurs; acting as regulatory enzymes, etc...

The study of the thermodynamics and mechanical properties of RNA structures is a non trivial issue. RNA is a molecule whose composition consists of a sequence of nitrogenous bases that are bound to a phosphate backbone, in the form of a single or double-stranded chain. Because of the presence of phosphates in the molecule backbone, the RNA molecule has a negative net charge, therefore the surrounding electrostatic phenomena play a very important role in the structure stabilization. In the biological environment (e.g. inside the cell) there are both monovalent and divalent ions as Na^{+} and Mg^{2+}. This circumstance highly affects duplex stability and therefore the secondary structure of RNA, and today we do not have a general tool to predict all RNA secondary structures. In fact, some fundamental thermodynamic information as specific vs. non-specific binding energies of ions has only been explored in the past few years [1].

Single-molecule techniques such as force spectroscopy (SMFS) are powerful tools which give us access to study biomolecules. The molecule concerning this study is a ribosomal RNA (rRNA), the *Three-Way Junction* (3WJ), from the central domain of 16S rRNA from E. coli, a structural RNA motif that acts as a substrate for the binding of the S15 protein. This RNA forms a competing misfolded structure that does not contain the binding site for S15 neither for specifically bind Mg, making it a very attractive candidate to study these interactions.

*Electronic address: xaviperezmore@gmail.com

II. DEVELOPING SECTIONS

A. Materials and methods

1. Optical tweezers

SMFS experiments were carried out in the Mini-Tweezers setup with temperature control described in detail in [2] and shown in figure 1.

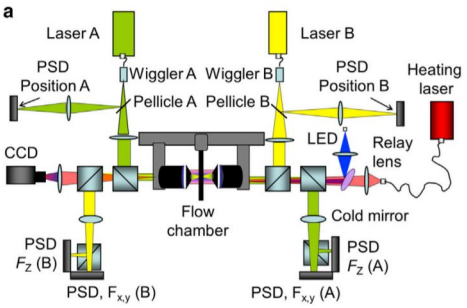

FIG. 1: Diagram of the Mini-Tweezers setup. Reproduced from [2].

Besides the ability to manipulate the molecule and the convenience of its force and spatial resolution, this device offers a precise measurement of the force by the change of light momentum. To achieve that, two counter-propagating lasers ($\lambda \sim 405$ nm) are focused to form the optical trap. Several position sensitive detectors (PSD) allow us to directly determine both the force and displacements of the optical trap. For temperature control, the device is thermalized at low temperatures and another laser ($\lambda \sim 1435$ nm) is used to heat the region of interest. However, in this case we have just performed experiments at ($\sim 7^{o}$C) and at room temperature ($\sim 25^{o}$C). A microfluidic chamber is placed between two microscope objectives. This chamber has three channels, a central one containing a glass micropipette which acts as the fixed point for our pulling experiment along with

two dispenser tubes that connect two auxiliary channels to the main one.

The instrument has been calibrated by two methods for each magnitude: position and force. The force measurements have been calibrated first by checking Stokes' law. Position was calibrated then using a force-feedback protocol while moving a bead with the micropipette. The tweezers were finally calibrated by pulling a known ds-DNA molecule, λDNA (24kbp), which shows a transition overstretching at a known force ($\sim$ 67 pN) [3].

2. *Molecular construction and experimental conditions*

The 3WJ is a short RNA molecule composed of 77 nucleotides (or bases). It is covalently bound to two hybrid RNA-DNA handles of $\sim$ 500 bases each. A detailed description of how to synthesize this construction can be found in [4].

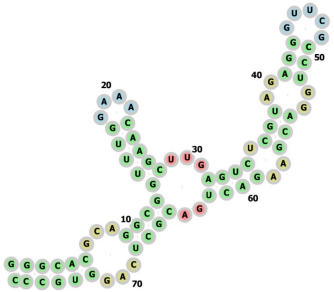

FIG. 2: Sequence of the 3WJ. Reproduced from [5].

As can be seen in figure 3 the molecule is manipulated thanks to two polystyrene microspheres of 2μm and 3μm and coated with streptavidin (SA bead) and anti-digoxigenin (AD), respectively. These beads bind to the extremes of the handles, which are labelled with biotin on one hand and digoxigenin on the other. We have performed experiments in two different salt conditions, thus two different buffers were prepared. The buffer composition for the monovalent condition is: 10mM HEPES, 300mM NaCl, 1mM EDTA, 0.01 % NaN_3 while for the diovalent condition, it is: 10mM HEPES, 50mM NaCl, 4mM $MgCl_2$, 0.01 % NaN_3. Both buffers were adjusted with NaOH-HCl at pH 7.5 and 25^{o}C. The election of HEPES guarantees that pH is stable at 7^{o}C.
Pulling experiments are carried out in the previously described microfluidic chamber. By moving the optical trap, the SA bead is immobilized by suction in the tip of the chamber's micropipette, and the AD bead is trapped in the force gradient of the optical trap.

3. *Experimental protocol*

To set up the experiment, the molecular construction (RNA plus handles) is incubated along with the AD beads in a small volume ($\sim$ 20μL) of buffer for 30 minutes. Then, the sample is diluted to a volume of 1mL and a dilution of SA is prepared in parallel. After that, both dilutions are flushed into the microfluidic chamber through the auxiliary channels to the experimental area where the optical trap is formed. The system is then set as in fig 3. Once the setup is completed, the experiment is carried out by an automatic protocol that moves the optical trap so the molecule is pulled back and forth at a constant pulling speed v_0. The range of the protocol is set so the molecule unfolds before the trap motion changes direction, and folds again before it reaches the initial position. The position of the trap is measured by splitting a fraction of the light to other PSDs. Then, we denote as λ the distance between the fixed point and the center of the trap.

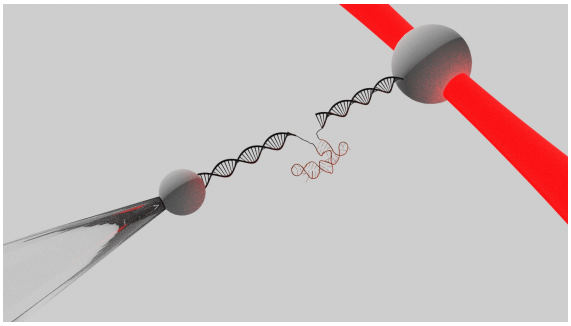

FIG. 3: Schematics of the experimental setup. Modified from [6].

The whole study revolves around the measurement of the rupture force at which the molecule unfolds (f_U) and refolds (f_F). Since it is a stochastic phenomenon, the results are the probability distributions of the unfolding and folding forces.

B. Modelling the system

1. *Elastic models for RNA*

Studying RNA mechanical properties requires of precise models for biomolecules elasticity, and physical models for polymers can be properly fitted [4]. Recalling the experiment, RNA transits from its folded configuration to its unfolded one by the action of force. In its folded state, the *freely-jointed chain* (FJC) model is used, which is a model based on the approach of the polymer as a union of linear monomers whose bonds motions are described as a random walk, and the estimation of the necessary energy to reorient the molecule [7],

$$x(f) = L_c \left(\coth\left(\frac{k_B T}{f \cdot b}\right) - \frac{k_B T}{f \cdot b} \right) \tag{1}$$

When the molecule unfolds to the single stranded configuration (ssRNA), its behaviour can be described using the*worm-like chain* model (WLC).

$$f(x) = \frac{k_B T}{4P}\left[\frac{1}{(1-x/L_c)^2} - 1 + \frac{4x}{L_c}\right] \quad (2)$$

where P is the persistence length and L_c is the molecular contour length. L_c is calculated as $L_c = N \cdot d_b$, being d_b the average inter-phosphate distance and N the number of bases in the molecule.

2. *Free energy and kinetic models*

Considering the unfolding process of the RNA molecule, all basepair bonds must be broken to unfold the molecule. Therefore it is reasonable to consider n, the number of nucleotides released from dsRNA to ssRNA (open bases), as the reaction coordinate. Then, it is possible to map all possible configurations to its free energy in the *Free Energy Landscape* (FEL):

$$G(n, f) = G_0^{(n)} + G_{\text{stretch}}(n, f) + G_{\text{orient}}(f) \quad (3)$$

Where $G_0^{(n)}$ is the free energy of formation at zero force of RNA secondary structure. These values can be obtained from open packages as Mfold. The reversible work to strectch the ssRNA is G_{stretch}, and G_{orient} the energy needed to orient the double helix of the folded configuration. A representation of the FEL for the 3WJ native structure is shown in fig 4.

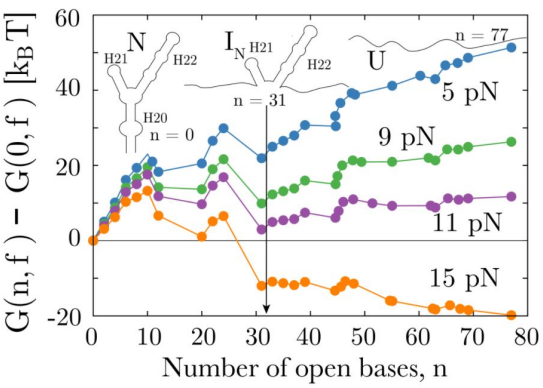

FIG. 4: Free energy landscape of the 3WJ. Reproduced from [8].

As can be seen, the FEL is highly influenced by the applied force, to the extent it that determines whether the transition occurs. As it is increased, the unfolded configuration is favored. Another local minima can be observed, specially at 31 open bases. This FEL coordinate is consistent with an intermediate state I_N that appears when the molecule refolds.

On the other hand, local maxima along the FEL can be interpreted as kinetic barriers in the unfolding reaction. According to this analogy, kinetic models can be applied. The Bell-Evans model (4) (5) portrays a two-state system with a force independent energetic barrier, and considers the modification of the free energy landscape by the applied mechanical force

$$k_{F\to U} = k_m \exp\left(\frac{f x_F}{k_B T}\right) \quad (4)$$

$$k_{U\to F} = k_m \exp\left(\frac{\Delta G_{FU} - f x_U}{k_B T}\right) \quad (5)$$

being k_m the kinetic rate for the unfolding reaction when no force is applied, and ΔG_{FU} the free energy variation from the folded to the unfolded state.

In order to match our mechanical unfolding experiment in this framework, the following steps are taken to determine the kinetic rates. During pulling experiments, unfolding and refolding transitions can be treated as a first order Markov process, and survival probabilities can be obtained from rupture forces integrating their distributions along the force axis as:

$$P_F(f) = 1 - \int_0^f \rho(f_U) f_U \;;\; P_U(f) = \int_0^f \rho(f_F) f_F \quad (6)$$

The kinetic rates can be calculated from the survival probabilities as:

$$k_{F\to U} = -r \frac{1}{P_F(f)} \frac{dP_F(f)}{df} \quad (7)$$

$$k_{U\to F} = r \frac{1}{P_U(f)} \frac{dP_U(f)}{df} \quad (8)$$

being the loading rate $r = df/dt$. If we take logarithms on the BE kinetic rates, a linear behaviour versus f is obtained.

C. Results and discussion

Previous studies related the FDC patterns for both the native and misfolded structures [9]. Force-distance curves (FDCs) were obtained and we selected the ones corresponding the native structure. A sample of those traces is shown in figure 5.

In order to confirm that it is actually the correct FDC, both the unfolding and refolding forces were obtained. Then, the change of extension in each transition were calculated and the resulting $(\Delta\lambda, f)$ were fitted to a WLC model with parameters $d_b = 0.655$ nm and $P(T) = P_0\sqrt{T/T_0}$ [10] with $P_0 = 0.75$ nm [1] to obtain N, the number of bases released(absorbed) in the unfolding(refolding). For the unfolding transition ~ 77 bases were obtained in agree with the total length of the molecule as we expected from figure 4.

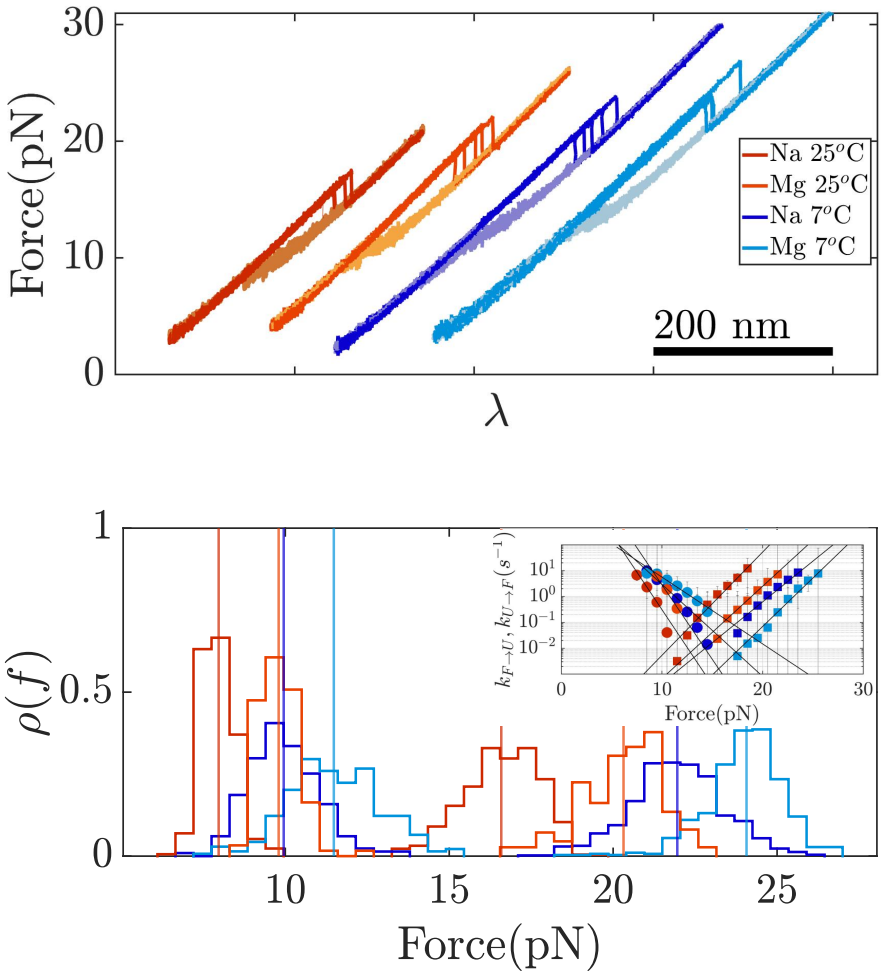

FIG. 5: **Top:** FDCs obtained from room temperature to cold (left to right) and for monovalent and divalent condition. **Bottom:**Representation of the refolding (left) and unfolding(right) forces histograms. **Inset**: Kinetic rates calculated from the equations 7, 8 .

Curves obtained at 25^{o}C show lower values for the unfolding forces, and for that reason, at 7^{o}C the protocol was modified to reach 40 pN instead of 20 pN as we did at room temperature. This effect can also be appreciated between different salt conditions at the same temperature. In the monovalent condition (i.e. only under the presence of Na^+ ions) the rupture event takes place around lower values than for the divalent condition.

The folding and unfolding events were identified and histograms are shown in figure 5. As anticipated before, mean unfolding forces are higher at lower temperatures. As for the refolding forces, it can be noticed that the effect of temperature is similar: the difference between the mean refolding force values for each condition is smaller. Kinetic rates from BE model also exhibits linear dependence with force, shown in figure 5 (inset).

To explain the temperature effect, recall the FEL for the 3WJ in the figure 4, that pictured how the force modified the landscape. At lower temperatures, the energy coming from the thermal bath, k_BT, is lower. In this case the kinetic barrier is crossed with lower probability, so the system needs to reach higher forces to unfold. Regarding the refolding forces, the principle works both ways so they shall be higher for lower temperatures as well. As can be seen also in figure 5(inset), also the crossing points of the linear fits from kinetic rates (i.e. the coexistence force) are shifted to higher forces at lower temperatures.

Furthermore, it is well known that Mg^{2+} is more effective at stabilizing RNA than Na^+ [1]. Buffers were prepared in a way that both salt conditions have similar ionic strengths, and differences can be attributed to the different types of cations in each condition.
In the 3WJ, the secondary structure of the native structure is highly affected by Mg^{2+}. The two helices following the junction are negatively charged, and under the presence of Mg^{2+}, the 3WJ undergoes a conformational

change in its tertiary structure, making the helices to approach. This conformational change is due to a specific binding of the cations to the junction. This effect is also observed in S15 binding, as reported years ago, by bulk methods [11] as well as with single-molecule fluorescence assays (FRET) [12].

Another fact observed that supports the stabilization role of both magnesium ions and low temperatures hypothesis is the appearance of two-force jump events in the unfolding curve under divalent condition and at 7^oC as illustrated in figure 6.

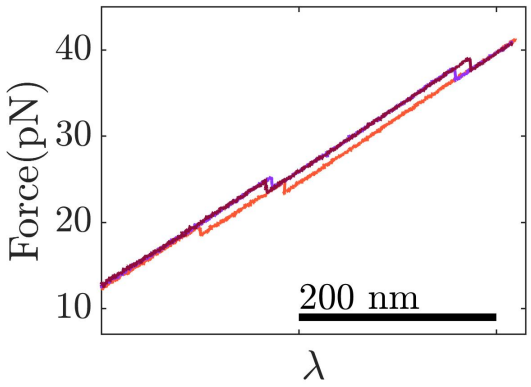

FIG. 6: FDCs showing a two-steps unfolding.

Trajectories compatible with the native FDCs of the 3WJ show this two-steps unfolding. Unfortunately, at the conditions set for this study, these events are rare so a detailed study requires further work. However we hypothesize that thanks to the combined effect of both cold temperatures and Mg^{2+}, an intermediate state is stabilized on the unfolding pathway of the native structure.

III. CONCLUSIONS

The experiments are successful and prove to be a very effective approach to study RNA thermodynamics. The results reassert the premise that the magnesium ions stabilize the molecule, likewise cold temperatures do. Even though the analysis of these conditions is mostly empiric, in the light of these results a wide range of possibilities opens.

The observation of the intermediate unfolding state under these conditions also raises a lot of questions as for the complexity of the RNA structures when undergoing the transition.

For future studies, it would be interesting to reproduce the experiment at higher concentrations of Mg^{2+} in order to gather a significant amount of data from this intermediate state. Moreover, the temperature effect could be further tested, to the extent of the physiological temperature (37^oC) for example, by means of the thermalizing laser.

Acknowledgments

I am very grateful to Felix Ritort and everyone in the Small Biosystems Lab for the opportunity to perform the experiments and the help provided. I would like to specially thank my advisor, Jaime Aspas Cáceres, for his teaching skills and for making this experience very enjoyable. Finally, thanks to my family and friends for their support.

[1] C. V. Bizarro, A. Alemany, and F. Ritort, Nucleic acids research **40**, 6922 (2012).
[2] S. De Lorenzo, M. Ribezzi-Crivellari, J. R. Arias-Gonzalez, S. B. Smith, and F. Ritort, Biophysical journal **108**, 2854 (2015).
[3] J. Gieseler, J. R. Gomez-Solano, A. Magazzù, I. P. Castillo, L. P. García, M. Gironella-Torrent, X. Viader-Godoy, F. Ritort, G. Pesce, A. V. Arzola, et al., Adv. Opt. Photon. **13**, 74 (2021).
[4] J. Camuñas i Soler, Ph.D. thesis, Universitat de Barcelona (2015).
[5] Á. Martínez Monge et al., Ph.D. thesis, Universitat de Barcelona (2019).
[6] J. Aspas Cáceres, I. Pastor, and F. Ritort, 7th International Iberian Biophysics Congress. Coimbra, PT. (2021).
[7] J. Camunas-Soler, M. Ribezzi-Crivellari, and F. Ritort, Annual review of biophysics **45**, 65 (2016).
[8] A. Monge, I. Pastor, C. Bustamante, M. Manosas, and F. Ritort (Unpublished).
[9] M. Manosas, I. Junier, and F. Ritort, Physical Review E **78**, 061925 (2008).
[10] W. Stephenson, S. Keller, R. Santiago, J. E. Albrecht, P. N. Asare-Okai, S. A. Tenenbaum, M. Zuker, and P. T. Li, Physical Chemistry Chemical Physics **16**, 906 (2014).
[11] R. T. Batey and J. R. Williamson, Rna **4**, 984 (1998).
[12] T. Ha, X. Zhuang, H. D. Kim, J. W. Orr, J. R. Williamson, and S. Chu, Proceedings of the National Academy of Sciences **96**, 9077 (1999).